

# Fast estimation of posterior probabilities in change-point analysis through a constrained hidden Markov model

The Minh Luong\*, Yves Rozenholc, and Gregory Nuel

*MAP5, Université Paris Descartes, 45 rue des Saints-Pères, 75006  
Paris, France*

July 2012

## Abstract

The detection of change-points in heterogeneous sequences is a statistical challenge with applications across a wide variety of fields. In bioinformatics, a vast amount of methodology exists to identify an ideal set of change-points for detecting Copy Number Variation (CNV). While considerable efficient algorithms are currently available for finding the best segmentation of the data in CNV, relatively few approaches consider the important problem of assessing the uncertainty of the change-point location. Asymptotic and stochastic approaches exist but often require additional model assumptions to speed up the computations, while exact methods have quadratic complexity which usually are intractable for large datasets of tens of thousands points or more. In this paper, we suggest an exact method for obtaining the posterior distribution of change-points with linear complexity, based on a constrained hidden Markov model. The methods are implemented in the R package *postCP*, which uses the results of a given change-point detection algorithm to estimate the probability that each observation is a change-point. We present the results of the package on a publicly available CNV data set

---

\*e-mail: [the-minh.luong@parisdescartes.fr](mailto:the-minh.luong@parisdescartes.fr); Corresponding author

( $n = 120$ ). Due to its frequentist framework, *postCP* obtains less conservative confidence intervals than previously published Bayesian methods, but with linear complexity instead of quadratic. Simulations showed that *postCP* provided comparable loss to a Bayesian MCMC method when estimating posterior means, specifically when assessing larger-scale changes, while being more computationally efficient. On another high-resolution CNV data set ( $n = 14,241$ ), the implementation processed information in less than one second on a mid-range laptop computer.

## 1 Introduction

The detection of *change-points* in heterogeneous sequences is a statistical challenge with many applications in fields such as finance, reliability, signal analysis, neurosciences and biology (Pinkel et al., 1998; Snijders et al., 2001). In bioinformatics in particular, a vast amount of methodology (Olshen et al., 2004; Fridlyand et al., 2004; Hupé et al., 2004) exists for identifying an ideal set of change-points in data from array Comparative Genomic Hybridization (aCGH) techniques, in order to identify Copy Number Variation (CNV).

A typical expression of the change-point problem is as follows, given data  $X = (X_1, X_2, \dots, X_n)$  of real-valued observations,  $(S_1, \dots, S_n)$  corresponding segment indices of the observations, and  $\mathcal{M}_K$  as the set of all possible combinations of  $S$  for fixed  $K \geq 2$  number of segments. The goal is to find the best partitioning  $S \in \mathcal{M}_K$  into  $K$  non-overlapping intervals, assuming that the distribution is homogeneous within each of these intervals.

For  $K$  segments of contiguous observations, the *segment-based model* expresses the distribution of  $X$  given a segmentation  $S \in \mathcal{M}_K$  as:

$$\mathbb{P}(X|S; \theta) = \prod_{i=1}^n g_{\theta_{S_i}}(X_i) = \prod_{k=1}^K \prod_{i, S_i=k} g_{\theta_k}(X_i) \quad (1)$$

where  $g_{\theta_k}(\cdot)$  is the parametric, or emission, distribution (e.g.: normal or Poisson) of the observed data with parameter  $\theta_k$ ,  $\theta = (\theta_1, \dots, \theta_K)$  is the global parameter, and  $S_i$  is the segment index at position  $i$ . For example, if  $n = 5$ ,  $K = 2$ , and with change-point located between positions 2 and 3, then  $S = (1, 1, 2, 2, 2)$ .

Introducing a prior distribution  $\mathbb{P}(S)$  on any  $S \in \mathcal{M}_K$  obtains a posterior distribution of the segmentation:

$$\mathbb{P}(S|X; \theta) = \frac{\mathbb{P}(X|S; \theta)\mathbb{P}(S)}{\sum_R \mathbb{P}(X|R; \theta)\mathbb{P}(R)}. \quad (2)$$

For a uniform prior, set  $\frac{1}{\mathbb{P}(S)} = \binom{n-1}{K-1} = |\mathcal{M}_K|$ .

A common alternative to the above segmentation procedure is to consider an unsupervised hidden Markov model (HMM). Assuming that  $S$  is a Markov chain of hidden states, this approach (Rabiner, 1989) can be thought of as being *level-based*, with the parameter of the  $k^{\text{th}}$  segment takes its value in the set of  $L \geq 1$  levels<sup>1</sup>:  $\{\theta_1, \theta_2, \dots, \theta_L\}$ . This simply is equivalent to the model defined by Equation (1), with the noticeable difference that  $S \in \{1, 2, \dots, L\}^n$ . With this level-based approach  $K \geq L$  in general, and the HMM is unconstrained in the sense that transitions are possible between any pair of states. This is an appropriate model when the conditional distribution within a given segment of contiguous observations may be shared among other segments. While the unconstrained HMM is preferable in many practical situations, the segment-based model requires less assumptions and is thus a more general model.

A convenient feature of these HMM approaches is in computing efficiently the posterior distribution  $\mathbb{P}(S|X; \theta)$  in  $O(L^2n)$  using classical forward-backward recursions (Durbin et al., 1998), making them suitable for handling large datasets. This paper focuses on using an computationally efficient exact procedure to characterize the uncertainty  $\mathbb{P}(S|X; \theta)$  of the estimated change-point locations using a hidden Markov model adapted to the conventional segmentation model as previously described. We exploit the effectiveness of the level-based HMM approach through a constrained HMM corresponding *exactly* to the above segment-based model, providing a fast algorithm for computing  $\mathbb{P}(S|X; \theta)$ .

We develop this posterior distribution procedure as change-point assessment in practical applications becomes more challenging from a computational point of view. For example, emerging high-throughput technologies are producing increasingly large amounts of data for CNV detection. For finding the exact posterior distribution of change-points  $\mathbb{P}(S|X; \theta)$ , Guédon (2007) suggested an algorithm in  $O(Kn^2)$ , while Rigai et al. (2011) considered the same quantity in a Bayesian framework with the same complexity. However, the complexity of these approaches provides for very slow processing for large datasets with sequences of tens of thousands or more. Other estimates generally focus on asymptotic behavior whose conditions are delicate due to the discreteness of the problem (Bai and Perron, 2003; Muggeo, 2003), on bootstrap techniques (Hušková and Kirch, 2008) and on stochastic methods such as particle filtering (Fearnhead and Clifford, 2003), recursive sampling (Lai et al., 2008), and Markov chain Monte Carlo

---

<sup>1</sup>Similar to the segment-based model, the choice of  $L$  is critical and is usually addressed through penalized criteria.

(Erdman and Emerson, 2008). Furthermore, many of the faster stochastic algorithms assume normal error structure to speed up the estimation procedures and are thus more difficult to adapt to non-normal data (Lai et al., 2008; Erdman and Emerson, 2008).

Section 2 presents a summary of current change-point methods, the constrained HMM algorithm and a description of the accompanying *R* statistical package, Section 3 implements the methods on a published array CGH data set and compares with published results, Section 4 presents examples of simple simulated data sets with comparisons between methods, Section 5 shows an illustrative example of the methods on a larger scale SNP array data set, while Section 6 includes a discussion.

## 2 Methods

### 2.1 Current change-point detection methods

A considerable amount of literature focuses on detecting the ideal number or set of change-point locations. For CNV detection, Fridlyand et al. (2004) developed a discrete HMM to map the number of states and the most likely state at each position. Observations where state transitions are most likely to occur indicate change-points. Various extensions to this HMM approach include various procedures such as merging change-points (Willenbrock and Fridlyand, 2005) and specifying prior transition matrices (Marioni et al., 2006) to improve the results, and simultaneous identification of CNV across multiple samples (Shah et al., 2009). HMM-based implementations for dealing with higher-resolution data for current array technologies include those from Colella et al. (2007); Wang et al. (2007).

A wide amount of segment-based approaches for identifying CNV in genomics data have also been explored. Olshen et al. (2004) introduced an extension of binary segmentation through a non-parametric approach, using permutation rather than parameter estimation to test for change-points. This algorithm requires data smoothing and pruning to improve computation time and change-point detection for very large sequences. To speed up this computationally-intensive process, Venkatraman and Olshen (2007) introduced adjusted p-values and stopping rules for the permutations. Hupé et al. (2004) introduced a likelihood-based approach to estimate parameters in a normal Gaussian model after adaptive weights smoothing. Hsu et al. (2005) proposed a wavelet-based change-point detection procedure with data smoothing, while Eilers and De Menezes (2005) introduced a quantile

approach to smoothing. Willenbrock and Fridlyand (2005); Lai et al. (2005) summarized and compared the various segmentation approaches for aCGH data.

To estimate the number of segments,  $K$ , Zhang and Siegmund (2007) extended an earlier method including a modified Bayes Information Criterion to adjust for the number of change-points using a recursive procedure. Comte and Rozenholc (2004) described a least squares minimization procedure with a penalization criterion for the number of contrasts, while Picard et al. (2005) implemented an adaptive method for estimating the location and number of change-points, with penalization terms for likelihoods.

## 2.2 Constrained HMM

Let us assume that  $S$  is a heterogeneous Markov chain over  $\{1, 2, \dots, K, K+1\}$  (where  $K+1$  is a “junk” state only considered for consistency reasons) such as  $\mathbb{P}(S_1 = 1) = 1$  and with the following transitions: for all  $2 \leq i \leq n$ , and  $1 \leq k \leq K$  we have  $\mathbb{P}(S_i = k | S_{i-1} = k) = 1 - \eta_k(i)$  and  $\mathbb{P}(S_i = k+1 | S_{i-1} = k) = \eta_k(i)$ . For consistency, choose  $\mathbb{P}(S_i = K+1 | S_{i-1} = K+1) = 1$ . For example, if  $n = 5$ ,  $K = 2$ , and  $S = (1, 1, 2, 2, 2)$  then  $\mathbb{P}(S) = (1 - \eta_1(2))\eta_2(3)(1 - \eta_2(4))(1 - \eta_2(5))$ . With this Markov chain, it is clear that  $\{S \in \mathcal{M}_K\} = \{S_n = K\}$ .

In the particular case where the Markov chain is homogeneous with  $\eta_k(i) = \eta \in ]0, 1[$  for all  $k$  and  $i$ ,  $\mathbb{P}(S) = (1 - \eta)^{n-K} \eta^{K-1}$  for all  $S \in \mathcal{M}_K$ <sup>2</sup>. In other words, only positive state jumps of  $+1$  are possible. Therefore  $\mathbb{P}(S | S \in \mathcal{M}_K) = 1/|\mathcal{M}_K|$ , which corresponds to the canonical choice of a uniform prior on  $\mathcal{M}_K$ . Note that a choice of different transition coefficients  $\eta_k(i)$  allows us to specify informative priors.

## 2.3 Forward-backward procedure and posterior probabilities

The constrained HMM provides a framework for additional inference on the uncertainty in the estimated change-point model; in particular, after obtaining the segmentation from any previous procedure, we can obtain confidence intervals around each of the identified change-points. In terms of practical applications, this approach is helpful when dealing with situations where both very short and very long segments may be present, and the exact location of change-points may not be identifiable.

---

<sup>2</sup>Note that the particular value of  $\eta$  does affect  $\mathbb{P}(S)$  but has no effect whatsoever on  $\mathbb{P}(S | S \in \mathcal{M}_K)$  of the chosen segmentation  $S$ . We can therefore safely make an arbitrary choice like  $\eta = 0.5$  for practical computations.

The forward-backward algorithm (Rabiner, 1989), also known as posterior encoding, is a recursive algorithm that can estimate the posterior probabilities of each observation  $i$  being in a particular hidden state  $S_i$ , and being a change-point such that  $S_i \neq S_{i-1}$ . The algorithm is of complexity  $O(Kn)$  for  $K$  segments and  $n$  observations; the sparse transition matrix between states reduces the  $O(K^2n)$  complexity of the classical forward-backward algorithm. A summary of this algorithm and other inferential procedures involved in HMM estimation is in Cappé et al. (2005).

We define the forward and backward quantities as follows, for observation  $i$  and state  $k$ :

For  $1 \leq i \leq n-1$ :

$$F_i(k) = \mathbb{P}(X_{1:i} = x_{1:i}, S_i = k) \quad (3)$$

$$B_i(k) = \mathbb{P}(X_{i+1:n} = x_{i+1:n}, S_n = K | S_i = k) \quad (4)$$

We obtain the forward quantities by recursion through the following formulae:  
Forward:

$$F_1(k) = \begin{cases} g_{\theta_1}(x_1) & \text{if } k = 1 \\ 0 & \text{else} \end{cases} \quad (5)$$

$$\begin{aligned} F_i(k) &= \sum_{\ell} F_{i-1}(\ell) \mathbb{P}(S_i = k | S_{i-1} = \ell, S \in \mathcal{M}_K) g_{\theta_k}(x_i) \\ &= [F_{i-1}(k)(1 - \eta_k(i)) + \mathbf{1}_{k>1} F_{i-1}(k-1) \eta_k(i)] g_{\theta_k}(x_i) \end{aligned} \quad (6)$$

where  $g_{\theta_k}(x_i)$  is the density function of the chosen emission distribution  $g$  with parameter  $\theta_k$ , when  $k$  is the underlying segment for observation  $i$ .

We use a similar recursive procedure to obtain the backward quantities:

Backward:

$$B_{n-1}(k) = \begin{cases} \eta_K(n) g_{\theta_K}(x_n) & \text{if } k = K-1 \\ (1 - \eta_K(n)) g_{\theta_K}(x_n) & \text{if } k = K \\ 0 & \text{else} \end{cases} \quad (7)$$

$$\begin{aligned} B_{i-1}(k) &= \sum_{\ell} \mathbb{P}(S_i = \ell | S_{i-1} = k, S \in \mathcal{M}_K) g_{\theta_{\ell}}(x_i) B_i(\ell) \\ &= (1 - \eta_k(i)) g_{\theta_k}(x_i) B_i(k) + \mathbf{1}_{k<K} \eta_{k+1}(i) g_{\theta_{k+1}}(x_i) B_i(k+1) \end{aligned} \quad (8)$$

To obtain the posterior probabilities of the state  $S_i = k$  at position  $i$ , we note

that :

$$\mathbb{P}(X_{1:n} = x_{1:n}, S \in \mathcal{M}_K) = F_1(1)B_1(1) \quad (9)$$

$$\mathbb{P}(S_i = k | X_{1:n} = x_{1:n}, S \in \mathcal{M}_K) = \frac{F_i(k)B_i(k)}{F_1(1)B_1(1)}. \quad (10)$$

The constrained HMM estimates the probability of changing state while being at state  $S_i = k$  at observation  $i$  as:

$$\mathbb{P}(S_i = k | X_{1:n} = x_{1:n}, S_{i-1} = k-1, S \in \mathcal{M}_K) = \frac{B_i(k)\eta_{k-1}(i)g_{\theta_k}(x_i)}{B_{i-1}(k-1)}. \quad (11)$$

We can sample a vector of length  $K-1$  change-points from the original data set through these quantities, and afterwards generate a new vector of observed data through the chosen emission distributions. The posterior probability of the  $k^{\text{th}}$  change-point occurring after observation  $i$ , or in other words  $i+1$  being the first observation in the  $k+1^{\text{th}}$  segment, is:

$$\begin{aligned} \mathbb{P}(CP_k = i | X_{1:n} = x_{1:n}, S \in \mathcal{M}_K) &= \mathbb{P}(S_i = k, S_{i+1} = k+1 | X_{1:n} = x_{1:n}, S \in \mathcal{M}_K) \\ &= \frac{F_i(k)\eta_k(i+1)g_{\theta_{k+1}}(x_{k+1})B_{i+1}(k+1)}{F_1(1)B_1(1)} \end{aligned} \quad (12)$$

The accuracy of these posterior probabilities relies on the ability of the preceding change-point model to provide proper initial estimates of the number of and locations of the change-points, as they are crucial in selecting the  $\theta_k$  parameters used in the forward-backward procedures.

Maximum *a posteriori* estimation of the most probable set of change-points is also possible through the Viterbi algorithm (Viterbi, 1967) by modifying the forward quantities, with the Viterbi quantities chosen as  $V_i(k)$  for observation  $i$  and state  $k$ .

$$\begin{aligned} V_1(1) &= g_{\theta_1}(x_1), \\ V_i(1) &= V_{i-1}(1)(1 - \eta_1(i))g_{\theta_1}(x_i), \text{ if } i \geq 2, k = 1 \\ V_i(k) &= \max \{V_{i-1}(k-1)\eta_k(i), V_{i-1}(k)(1 - \eta_k(i))\} g_{\theta_k}(x_i), \text{ if } i, k \geq 2 \end{aligned}$$

We trace the path of indices  $k$  used to calculate  $V_{i,k}$  to get the set of change-points with highest posterior probability:

- $K-1^{\text{th}}$  change-point  $CP_{K-1}$ :  $i$  of  $V_i(K-1)$  used to calculate  $V_{i+1}(K)$
- $k^{\text{th}}$  change-point  $CP_k$ :  $i$  of  $V_i(k)$  used to calculate  $V_{i+1}(k+1)$  (where  $CP_k < CP_{k+1}$ ).

## 2.4 Statistics package `postCP`

We apply the preceding methods in the statistics package `postCP`, available on the CRAN website

<http://cran.r-project.org/web/packages/postCP>.

The forward and backward recursive algorithms are programmed in C++ to optimize the speed of the computationally-intensive process.

The following is a typical *R* command line for segmenting a sequence *LRR*, with a vector of length  $K - 1$  change-points (or last index of segments) *initseg*, and 95% confidence intervals. The options also save forward-backward and posterior change-point probabilities in the output, obtain the most likely set of change-points through the Viterbi algorithm, and generate 100 different vectors (each of length  $K - 1$ ) of change-point locations for generating data according to our change-point model.

```
postCP(data=LRR,seg=initseg,ci=0.95,viterbi=TRUE,nsamples=100)
```

The package also provides documentation for options on specifying a matrix of log-densities corresponding to any specified distribution of the data, and the prior specification of a matrix of transition probabilities.

## 3 Detecting copy number variation in array CGH breast cancer data

We apply the methods to a widely referenced data set from cell line BT474 from a breast cancer tumor (Snijders et al., 2001). The data consist of log-reference ratios signifying the ratio of genomic copies of test samples compared to normal. The goal is to segment the data into segments with similar copy numbers, with change-points corresponding to copy number aberrations pointing to possible genes of interest (Pinkel et al., 1998). We compare the results of `postCP` to the Bayesian confidence intervals previously published on the same data by Rigai et al. (2011), consisting of 120 observations from chromosome 10. The observations are sorted according to their relative position along chromosome 10.

We use a modification of the greedy least squares *K*-means algorithm (Hartigan and Wong, 1979) to obtain an initial segmentation for 3 and 4 segments (Table 1). The locations refer to the indices of the last observations of the first  $K - 1$  segments. Afterwards, we used *postCP* to obtain estimates of the forward and backward matrices in Section 2.3, and afterwards, estimates of the posterior



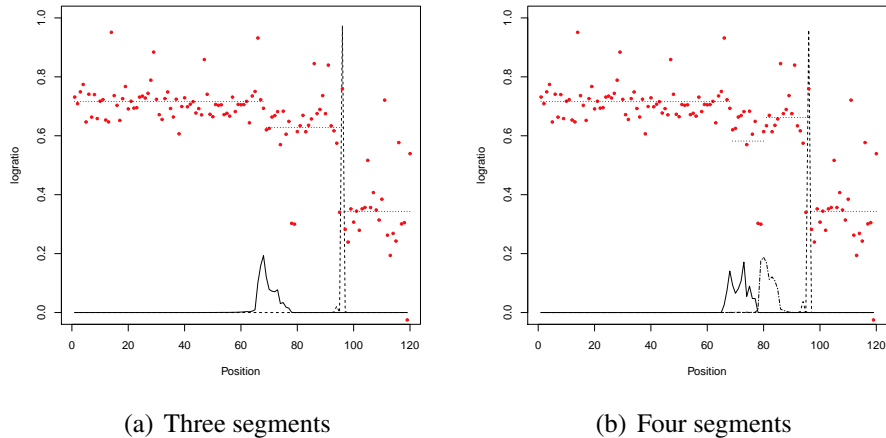


Figure 1: Plots of estimated posterior change-point probabilities for chromosome 10 data (Snijders et al., 2001). Dots are LRR data with horizontal lines representing the estimated means within segments scaled to the probability axes. (a) Posterior probabilities for three segments, first change-point initialized after  $i = 68$  is a solid line, 2nd initialized after  $i = 96$  is a dashed line. (b) Posterior probabilities for four segments, additional change-point after  $i = 80$  is a dotted-dashed line.

probabilities of the change-points being at each observation. We assumed a homoscedastic normal model for the observations.

Figure 1(a) displays the estimated posterior change-point probabilities of the aCGH data for three segments and Figure 1(b) for four segments. For both segmentations, the probability of the last change-point had a sharp peak close to 1.0. There is an additional change-point found at position 80 by the four segment model with a relatively high uncertainty. In both the 3- and 4-segment instances, the shapes of the change-point distributions are irregular due to the discreteness of the segmentation procedure.

At these predefined observations, the corresponding posterior change-point probabilities were higher than reported by Rigaiil, and confidence intervals were slightly narrower. This is expected, as Rigaiil's method uses a Bayesian framework that accounts for the uncertainty in the parameter estimates. In particular, the rightmost change-point estimation with both 3 and 4 segments had posterior probabilities above 0.95, while the corresponding posterior probabilities from the

Table 1: Change-point confidence intervals aCGH chromosome 10

CP #	$\Delta$ mean	Est location	95 % CI (postCP)	95% CI (Bayesian)
Three segments				
1	-0.22	68	66-76	64-78
2	-0.71	96	96-96	92-97
Four segments				
1	-0.34	68	66-76	66-78
2	-0.20	80	79-85	78-97
3	-0.80	96	96-96	91-112

Change-point estimates of aCGH data for chromosome 10 from Snijders et al. (2001), with (95% confidence interval), by *postCP* and Bayesian confidence intervals by Rigaiil et al. (2011). Narrower confidence intervals were found by *postCP*.

Bayesian method were closer to 0.5.

We also can use *postCP* to obtain a joint sample of an entire set of change-points from the original data using the constrained HMM model. Using *postCP*, we sampled 10,000 data sets using (11). As seen in Figure 2, the histogram of the generated locations for the first two change-points closely approximates the posterior change-point probabilities found by *postCP*. Though there is little overlap between the estimated confidence intervals for the first two change-points, there was still a small but non-zero empirical Pearson correlation ( $r = 0.123, p < 0.001$ ) between the simultaneously generated first and second change-point locations. On the other hand, there was no association between the third generated change-point and the other two change-points, an expected result since their confidence intervals do not overlap.

## 4 Change-point data simulations and comparisons

In this section we consider different change-point situations to compare the ability of the methods in assessing uncertainty. In this section, we use a loss function to assess the ability of the change-point methods in estimating the posterior mean of each observation ( $i = 1, \dots, n$ ). For normally distributed data, we quantify loss through the mean square error (MSE). We define  $MSE = \sum_i (\hat{\theta}(i) - \theta_{S_i})^2$ , where

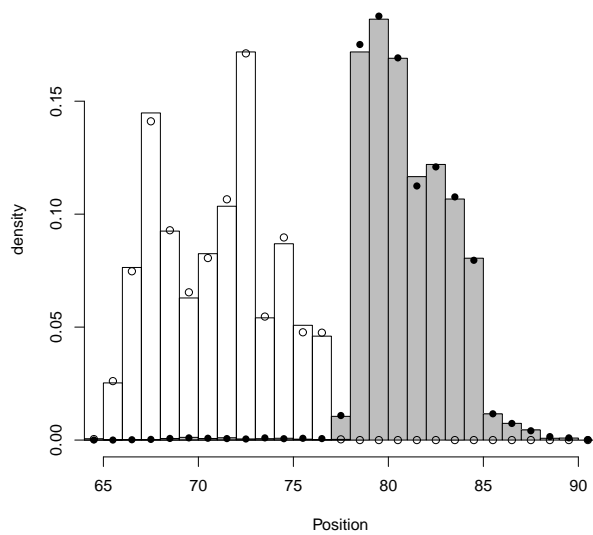


Figure 2: Histogram of locations of the first two change-points, randomly and simultaneously generated by *postCP* for 10,000 sets, for data from Snijders et al. (2001). The frequencies of the first change-point from the simulations are in white boxes, of the second in gray boxes. The estimated change-point probabilities by the forward-backward algorithm for the first change-point are in white dots, for the second change-point in black. The randomly generated change-points are close to those estimated by *postCP*.

$\theta_{S_i}$  are the true underlying means for each observation. For non-normal data, we use the median absolute error (MAE) where  $MAE = \sum_{i=1}^n |(\hat{\theta}(i) - \theta_{S_i})|$ .

We obtain 4 different estimates for the posterior mean of each of the  $n$  observations as follows. The first two posterior mean estimates are from the Bayesian MCMC method implemented in the *bcp* package (Erdman and Emerson, 2008) and the circular binary segmentation method from the *DNAcopy* package (Olshen et al., 2004; Venkatraman and Olshen, 2007) in *R*, both at the default parameters.

We also use *postcp*, with initial change-points from the estimated change-point set found by *DNAcopy*, to estimate posterior probabilities of being in state  $k$  for each observation  $i$ ,  $P(S_i = k | X_{1:n} = x_{1:n}, S \in \mathcal{M}_K)$ , and segment means  $\hat{\theta}_k; k = 1, \dots, \hat{K}$ . The posterior mean of observation  $i$  is:

$$\hat{\theta}(i) = \sum_{k=1}^{\hat{K}} P(S_i = k | X_{1:n} = x_{1:n}, S \in \mathcal{M}_K; \hat{\theta}_k) \hat{\theta}_k.$$

To obtain another initial set of change-points for *postCP*, we use another greedy procedure for quick model selection as follows. First, we use the greedy least-squares minimizing algorithm for a fixed  $K$  number of segments to obtain an initial set of change-points. We then use the Viterbi algorithm to get the most probable set of change-points based on this initial set, and obtain the corresponding maximum likelihood estimates (MLEs) for the model parameters. The estimated number of segments  $\hat{K}$  is that which maximizes the Bayesian information criterion (BIC) (Schwarz, 1978; Picard et al., 2005),

$$BIC(K) = LL - K' \log(n),$$

with respect to the number of segments, where  $LL$  is the log-likelihood of the data, and  $K'$  is the number of parameters in the model. Posterior quantities are as previously described.

We simulated a sequence of  $n = 500$  observations with 6 change-points after  $i = (22, 65, 108, 219, 252, 435)$ . For normally distributed data, odd segments had mean  $\theta_0 = 0.0$  and even segments had various values of  $\theta_1$  with standard deviation 1.0. For Poisson data, odd segments had mean  $\theta_0 = 1.0$ . We implement these procedures on 1000 sets each of normal and Poisson distributed data for these 4 methods. Results in Table 2 report the MSE for normal data and MAE for Poisson data for different parameter values of  $\theta_1$ .

For normally distributed data and  $n = 500$ , *bcp* had lower MSE than the *postcp* estimates when the intersegmental differences, or differences between the even

Table 2: Average error of different change-point methods

		$n = 500$				$n = 10,000$			
$\theta_0$	$\theta_1$	cbs	cbs +postCP	greedy +postCP	bcp	cbs	cbs +postCP	greedy +postCP	bcp
normal distribution									
0.0	0.25	0.017	0.017	0.017	0.016	0.014	0.013	0.014	0.013
	0.50	0.058	0.055	0.054	0.045	0.021	0.018	0.025	0.015
	0.75	0.083	0.074	0.080	0.051	0.020	0.016	0.025	0.015
	1.00	0.068	0.055	0.074	0.052	0.018	0.014	0.022	0.015
	1.25	0.055	0.043	0.053	0.051	0.018	0.014	0.022	0.015
	1.50	0.050	0.039	0.043	0.047	0.017	0.013	0.021	0.014
	1.75	0.049	0.039	0.040	0.045	0.017	0.013	0.020	0.015
	2.00	0.047	0.037	0.037	0.043	0.015	0.012	0.019	0.014
	2.25	0.045	0.036	0.036	0.041	0.015	0.012	0.018	0.015
	2.50	0.042	0.034	0.034	0.039	0.014	0.011	0.017	0.017
Poisson distribution									
1.0	2.0	0.225	0.225	0.154	0.188	0.0438	0.045	0.051	0.062
	3.0	0.112	0.112	0.119	0.196	0.0451	0.045	0.050	0.057
	4.0	0.114	0.116	0.122	0.178	0.0469	0.047	0.050	0.055
	5.0	0.122	0.123	0.126	0.175	0.0477	0.046	0.051	0.057
	6.0	0.123	0.123	0.126	0.171	0.0519	0.051	0.052	0.066
	7.0	0.136	0.137	0.138	0.180	0.0529	0.053	0.055	0.080
	8.0	0.137	0.136	0.138	0.175	0.0497	0.049	0.053	0.091
	9.0	0.139	0.140	0.140	0.181	0.0540	0.054	0.056	0.114
	10.0	0.149	0.149	0.148	0.187	0.0546	0.055	0.058	0.150
	11.0	0.154	0.154	0.153	0.194	0.0548	0.055	0.055	0.175

Error of posterior means for different change-point uncertainty methods, in terms of Mean Square Error (MSE) for normally distributed observations and Median Absolute Error (MAE) for Poisson distributed observations.

and odd segments, were less than 1.0 standard deviations. This may be due to the frequentist nature of *postcp* using point estimates of change-point location to calculate MLEs, which may not have been accurate at lower intersegmental differences. However, at larger intersegmental differences, the methods relying on *postCP* actually had lower MSE than *bcp*. In particular, for larger intersegmental differences, the Bayesian method at the default parameters of *bcp* were overly conservative.

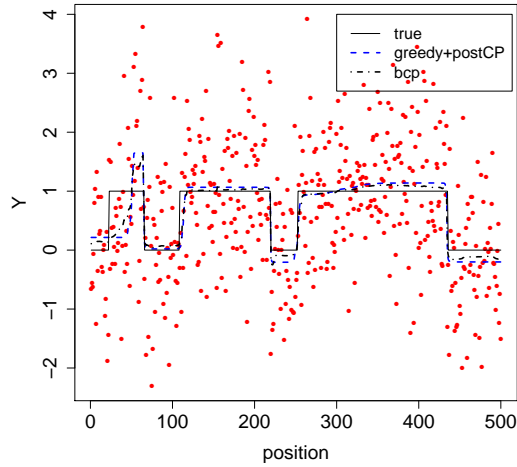
For illustrative purposes, Figures 3(a) and 3(b) compare the true values of the underlying means to those found from *greedy+postCP* and from *bcp* in one specific set of generated data. For true intersegmental differences of  $\Delta = \theta_1 - \theta_0 = 1.0$ , *bcp* had slightly lower MSE than *postCP*. Inaccurate locations from the greedy algorithm and BIC resulted in a greater amount of error from *postCP* compared to the relatively conservative posterior change-point probabilities from *bcp*. However, at  $\Delta = 2.0$ , *postCP* performed slightly better than *bcp*, as the greedy algorithm and BIC provided the correct number of segments and accurate initial change-point estimates to *postCP*.

For Poisson distributed data, the *postCP* based methods had lower MAE than *bcp*, showing the flexibility of the *postCP* procedure which can adapt to non-normal data.

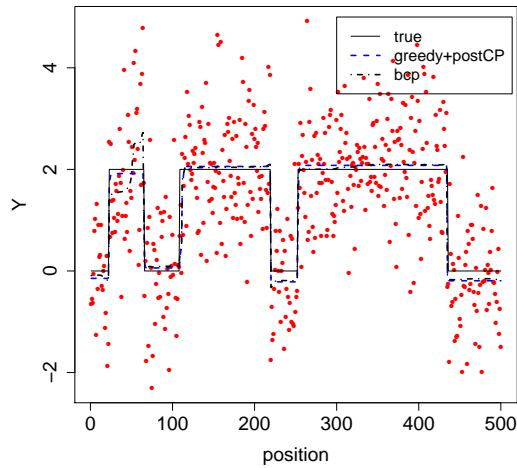
Figures 4(a) and 4(b) compare the true values of the underlying means for one set of Poisson data, for intersegmental differences of 2.0 and 4.0, respectively. It is evident that *postCP* provides more appropriate posterior mean estimates as *bcp* is not adapted for non-normally distributed data, with highly irregularly-shaped curves for the posterior means.

We also repeat the procedure on a larger sequence of 10,000 observations, with 39 change-points randomly selected from a uniform distribution within these observations, such that no segment is less than 25 observations long. While there is less deviation in the posterior means due to larger segment sizes, the problem of estimating the number and location of change-points is made more difficult. For normal data using *postCP* after initialization by *cbs* showed similar patterns to those from  $n = 500$ , obtaining lower MSE than *bcp* other than for very small intersegmental differences. However, using *postCP* after the greedy algorithm and BIC did not fare as well. Due to the larger amount of change-points, a more effective change-point location estimator than greedy least squares is recommended in these situations.

The exact *postCP* algorithms also provided some computational advantages in terms of model selection over the Bayesian MCMC method *bcp*, which also has linear complexity. For  $n = 500$ , the entire model selection procedure averaged

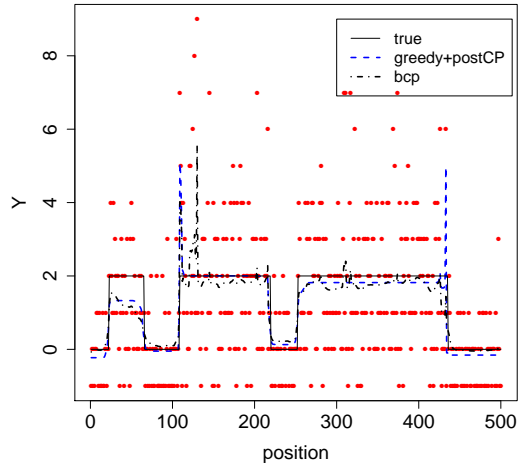


(a)  $\theta_1 - \theta_0 = 1.0$

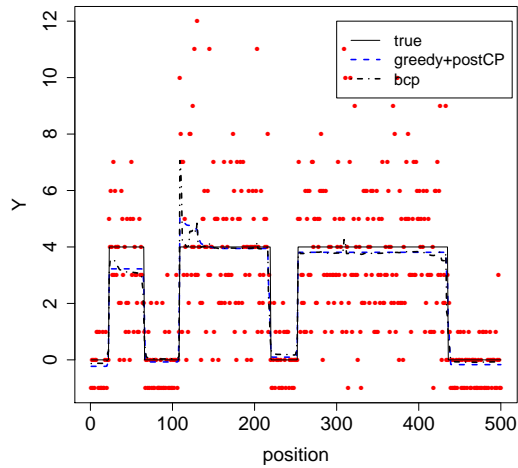


(b)  $\theta_1 - \theta_0 = 2.0$

Figure 3: Plot of sample data  $n = 500$  from normal distribution in Table 2. Underlying means in thin solid black lines, posterior means estimated by *greedy+cp* in dashed blue lines and by *bcp* in thick dash-dotted black lines. (a) Intersegmental differences of 1.0 SD, MSE for *bcp* 0.043, for *greedy+postcp* 0.066. The first change-point is not located precisely (at  $i = 50$ ) by the greedy method, with an extra change-point at  $i = 299$  from BIC. *bcp* provided more conservative estimates slightly closer to true values in these regions. (b) Intersegmental differences of 2.0 SD, MSE for *bcp* was 0.053, for *greedy+postcp* was 0.040. More precise *greedy+postcp* estimates after correct first change-point was entered.



(a)  $\theta_1 - \theta_0 = 2.0$



(b)  $\theta_1 - \theta_0 = 4.0$

Figure 4: Plot of sample data  $n = 500$  from the Poisson distribution used in Table 2. Underlying means in thin solid black lines, posterior means estimated by *greedy+cp* in dashed blue lines and by *bcp* in thick dash-dotted black lines. In both situations, the Bayesian estimates from *bcp* provided irregularly shaped posterior mean curves. (a)  $\theta_0 = 1$  and  $\theta_1 = 3$ , median absolute error for *bcp* was 0.205, for *greedy+postcp* was 0.172. (b)  $\theta_0 = 1$  and  $\theta_1 = 5$ , MSE for *bcp* was 0.180, for *greedy+postcp* was 0.175.



0.07 seconds with the greedy+postcp model selection procedure, 0.09 seconds for cbs+postcp and 0.9 seconds for *bcp*. For  $n = 10,000$ , the respective runtimes were 1.37 seconds for cbs+postcp together and 15.7 seconds for *bcp*.

## 5 Detecting copy number variation in SNP array colorectal cancer data

To illustrate the efficiency of the constrained HMM model, we apply the methods to a copy number variation profile obtained through current SNP (single nucleotide polymorphism) microarray technology (Staaf et al., 2008). The data contain 261,563 SNPs across the genome obtained from an Affymetrix chip from a colorectal cancer tumor cell line (De Roock et al., 2010) with intensities providing information regarding mutations, specifically duplications and deletions. After normalization, the log of the intensities in the tumor sample were compared to normal values, obtained from a reference sample, to obtain the log-reference ratios (LRR) across each of 23 chromosomes.

We use the circular binary segmentation (CBS) procedure implemented in a widely used segmentation package, DNACopy (Olshen et al., 2004; Venkatraman and Olshen, 2007) for the statistics software *R*. This package obtains an initial estimate of change-points in LRR, for each of the 23 chromosomes in tumor sample 103. We ran DNACopy, after smoothing, at the default parameters of  $\alpha = 0.01$ . Table 3 displays the best segmentation found within for 14,241 SNPs from chromosome 10. This chromosome was selected since both small (second) and large (tenth) segments were found, with adjacent segment differences ranging from 0.04 to 0.58 (Figure 5).

We ran *postCP* using the set of change-points identified by DNACopy as initial segmentation to obtain estimates of the posterior probabilities of the change-points being at these ten locations. We assumed a homoscedastic normal model for the observations. The forward-backward algorithm was practically instantaneous (less than 0.1 seconds) for this sequence of over 14,000 observations on a mid-range dual-core 2.5 GHz, 4GB RAM laptop PC. Not surprisingly, the most narrow confidence intervals, and most precise change-point estimates, were found for larger differences (Table 4). Of the ten estimated change-points, six separated segments whose means differed by greater than one standard deviation; these points all were found to have posterior change-point probabilities greater than 0.5. Eight of the ten change-points from DNACopy had the highest posterior

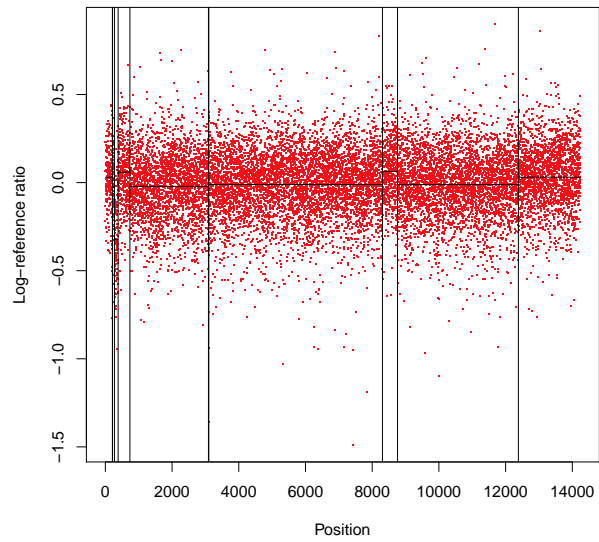


Figure 5: Plot of 14,241 log-reference ratios (LRR) for chromosome 10. Horizontal lines are the estimated means within segments, vertical lines are the ten change-points estimated by DNACopy.

Table 3: Segmentation from CBS for chromosome 10

Segment	Start	End	Size	Mean
1	1	211	211	0.031
2	212	215	4	-0.552
3	216	273	58	-0.028
4	274	383	110	-0.322
5	384	736	353	0.060
6	737	3091	2355	-0.021
7	3092	3102	11	-0.477
8	3103	8308	5206	-0.011
9	8309	8760	452	0.064
10	8761	12383	3623	-0.011
11	12384	14241	1858	0.031

Best segmentation results from circular binary segmentation algorithm (Olshen et al., 2004). Information from  $K = 11$  segments, with index of start and end of segment, size of the segment, and the mean within the segment. The pooled standard deviation across the segments was  $\sigma = 0.188$ .

Table 4:

Change point	CP Est	Post Prob	$\Delta$ Mean	Size of confidence interval				
				ci:0.5	0.6	0.7	0.8	0.9
1	211	0.973	-0.582	1	1	1	1	1
2	215	0.918	0.523	1	1	1	1	1
3	273	0.556	-0.293	1	2	2	2	3
4	383	0.580	0.381	1	2	2	2	3
5	736	0.028 <sup>a</sup>	-0.081	31	37	46	53	61
6	3091	0.860	-0.456	1	1	1	1	2
7	3102	0.880	0.466	1	1	1	1	2
8	8308	0.050	0.075	21	30	50	91	132
9	8761	0.064	-0.075	15	21	48	63	78
10	12383	0.006 <sup>b</sup>	0.042	233	336	412	501	522

Information for 10 change-points identified within chromosome 10. The posterior probability of a change was at least 0.50 for all change-points with a moderate change ( $> \sigma = 0.188$ ), while wider confidence intervals were found when segment differences were smaller. <sup>a</sup>: point 721 had slightly higher change-point probability (0.031), <sup>b</sup>: point 11943 had slightly higher change-point probability (0.008).

change-point probabilities for their positions, with the exception of the fifth and tenth change-points whose probabilities were slightly lower than the respective maximum of their position.

Figure 6(a) displays the posterior change-point probabilities for the first five change-points. Given the much narrower segment lengths, and greater segment differences, the probabilities are much higher for the first four change-points than the fifth change-point, whose 90% confidence interval was greater than 60 SNPs wide. Figure 6(b) displays the posterior change-point probabilities for the tenth change-point, whose 90% confidence interval was greater than 500 SNPs wide. Note that the shapes of the change-point distributions are also highly irregular.

## 6 Discussion

A common point of interest in current genomics studies is to find genetic mutations pointing to phenotypes susceptible to diseases (Redon et al., 2006) such as

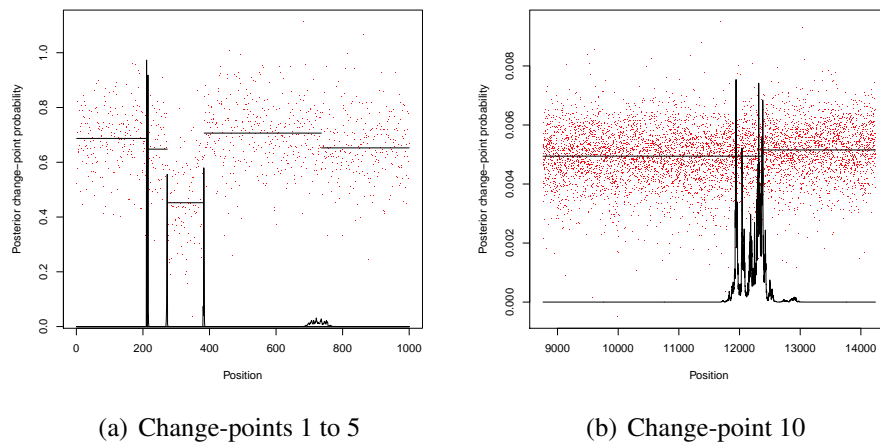


Figure 6: Plot of estimated posterior change-point probabilities. Dots are LRR data with horizontal lines the estimated means within segments scaled to the probability axes. (a) For first five change-points: The first four change-point estimates (SNPs at position: 211, 215, 273, 383) are precise, however there is a wide uncertainty around the fifth change-point (position: 736). (b) For tenth change-point: There is a very wide confidence interval for this change-point estimate. The change-point estimate from the CBS algorithm (position 12,383) is the fourth rightmost peak.

cancers or Type II diabetes. The use of change-point analysis for detecting copy number variation (CNV) is a critical step in the characterization of DNA, including tumoral genes associated with cancer. A CNV may aid in locating a genetic mutation such as a duplication or deletion in a cancerous cell that is a target for treatment. However, due to the often large nature of genomics data sequences it is often difficult to reliably identify CNVs. The latest technologies for detecting CNV, such as single nucleotide polymorphism (SNP) arrays, are able to produce sequences of tens or hundreds of thousands of observations.

This paper describes a procedure that extracts further useful information from segmenting large sequences such as those found in CNV detection in SNP array data. The unsupervised HMM, which is a level-based approach used in many current implementations, includes forward-backward calculations in linear time. However they are less flexible than segment-based methods, in part because they require prior transition probabilities between states that assume a geometric prior on segment lengths, which may be inappropriate in some situations. On the other hand, most segment-based methods can allow for a wider variety of specified priors, but in many situations are unfeasible due to their quadratic complexity for large data sets such as those generated by SNP arrays.

The described constrained HMM model's complexity of  $O(Kn)$  rather than  $O(Kn^2)$  enables it to handle very large data sets in reasonable time. The procedure allows for the estimation of the full joint distribution of change-points conditional to the observations, allowing for practical estimation of confidence intervals. In high-resolution data sets with change-points to be unlikely detected at the exact correct position, the confidence intervals may yield important information. In SNP array technology, the change-points need to be detected with high-precision and the differences between segments may not be very large. Additionally, overlapping confidence intervals across several different cell tumors or lines may identify associated copy number variations, and help in identifying similar disease phenotypes and treatments in patient subgroups.

The emission distribution  $g_{\theta}(x)$  of the observed data can also be easily specified in this constrained HMM procedure, unlike other implementations specifically developed for normally distributed large-scale data. The ability of *postCP* to easily adapt to a wide variety of distributions through the specification of the emission distribution is especially important with next-generation sequencing platforms often producing data that closely follows the Poisson or Negative Binomial distributions (Shen et al., 2011).

The described methods are a useful tool in the segmentation of large-scale sequences such as those involving CNVs, specifically when combined with any

current implementation designed for detecting an ideal set of change-points. For example, a fast dynamic programming algorithm of order  $O(n \log n)$  developed by Comte and Rozenholc (2004) obtaining an initial segmentation of the points is to be bundled in the *postCP* package. While the constrained HMM approach is sensitive to its starting point and tends to provide a local rather than global optimum if the initial starting points are misspecified, simulations in this paper showed that in practice, *postCP* provided estimates of posterior means that were comparable to, or sometimes better than, a currently implemented Bayesian MCMC method. This occurred in situations in which the Bayesian method was specifically designed, that is for assessing multiple change-points in normally distributed data.

A planned extension of our method is to combine the segment-based and level-based approaches by limiting possible values of segment parameters  $(\theta_1, \dots, \theta_K)$  to  $L \leq K$  different values. Further practical applications include more complex models to simultaneously model multiple datasets, or accounting for values from multiple patients and samples as random effects in a mixed model. Another practical extension is to handle multi-dimensional output, such as current technology for copy numbers (Staaf et al., 2008) that simultaneously includes LRR and baseline allelic frequency (BAF) data.

## Acknowledgements

We would like to thank Dr. Pierre Laurent-Puig of the INSERM S-775 biomedical laboratory of Paris Descartes for permitting us to use the colorectal cancer SNP array data used in our illustrative example on high-resolution data, and Mr. Mael Thépaut for providing the normalized data set. We would also like to thank Prof. Stéphane Robin and Dr. Guillem Rigail for providing us with the breast cancer data from cell line BT474 they used in the previous publication.

## References

- Bai, J., Perron, P., 2003. Computation and analysis of multiple structural change models. *Journal of Applied Econometrics* 18 (1), 1–22.
- Cappé, O., Moulines, E., Rydén, T., 2005. *Inference in hidden Markov models*. Springer Verlag.
- Colella, S., Yau, C., Taylor, J., Mirza, G., Butler, H., Clouston, P., Bassett, A.,

- Seller, A., Holmes, C., Ragoussis, J., 2007. QuantiSNP: an Objective Bayes Hidden-Markov Model to detect and accurately map copy number variation using SNP genotyping data. *Nucleic Acids Research* 35 (6), 2013.
- Comte, F., Rozenholc, Y., 2004. A new algorithm for fixed design regression and denoising. *Annals of the Institute of Statistical Mathematics* 56 (3), 449–473.
- De Roock, W., Claes, B., Bernasconi, D., De Schutter, J., Biesmans, B., Fountzilas, G., Kalogeras, K., Kotoula, V., Papamichael, D., Laurent-Puig, P., et al., 2010. Effects of KRAS, BRAF, NRAS, and PIK3CA mutations on the efficacy of cetuximab plus chemotherapy in chemotherapy-refractory metastatic colorectal cancer: a retrospective consortium analysis. *The Lancet Oncology* 11 (8), 753–762.
- Durbin, R., Eddy, S., Krogh, A., Mitchison, G., 1998. *Biological sequence analysis: Probabilistic models of proteins and nucleic acids*. Cambridge Univ Pr.
- Eilers, P., De Menezes, R., 2005. Quantile smoothing of array CGH data. *Bioinformatics* 21 (7), 1146–1153.
- Erdman, C., Emerson, J., 2008. A fast Bayesian change point analysis for the segmentation of microarray data. *Bioinformatics* 24 (19), 2143–2148.
- Fearnhead, P., Clifford, P., 2003. On-line inference for hidden Markov models via particle filters. *Journal of the Royal Statistical Society: Series B (Statistical Methodology)* 65 (4), 887–899.
- Fridlyand, J., Snijders, A., Pinkel, D., Albertson, D., Jain, A., 2004. Hidden Markov models approach to the analysis of array CGH data. *Journal of Multivariate Analysis* 90 (1), 132–153.
- Guédon, Y., 2007. Exploring the state sequence space for hidden Markov and semi-Markov chains. *Computational Statistics & Data Analysis* 51 (5), 2379–2409.
- Hartigan, J., Wong, M., 1979. Algorithm AS 136: A K-means clustering algorithm. *Journal of the Royal Statistical Society. Series C (Applied Statistics)* 28 (1), 100–108.
- Hsu, L., Self, S., Grove, D., Randolph, T., Wang, K., Delrow, J., Loo, L., Porter, P., 2005. Denoising array-based comparative genomic hybridization data using wavelets. *Biostatistics* 6 (2), 211–226.



- Hupé, P., Stransky, N., Thiery, J., Radvanyi, F., Barillot, E., 2004. Analysis of array CGH data: from signal ratio to gain and loss of DNA regions. *Bioinformatics* 20 (18), 3413–3422.
- Hušková, M., Kirch, C., 2008. Bootstrapping confidence intervals for the change-point of time series. *Journal of Time Series Analysis* 29 (6), 947–972.
- Lai, T., Xing, H., Zhang, N., 2008. Stochastic segmentation models for array-based comparative genomic hybridization data analysis. *Biostatistics* 9 (2), 290–307.
- Lai, W., Johnson, M., Kucherlapati, R., Park, P., 2005. Comparative analysis of algorithms for identifying amplifications and deletions in array CGH data. *Bioinformatics* 21 (19), 3763.
- Marioni, J., Thorne, N., Tavaré, S., 2006. BioHMM: a heterogeneous hidden Markov model for segmenting array CGH data. *Bioinformatics* 22 (9), 1144–1146.
- Muggeo, V., 2003. Estimating regression models with unknown break-points. *Statistics in Medicine* 22 (19), 3055–3071.
- Olshen, A., Venkatraman, E., Lucito, R., Wigler, M., 2004. Circular binary segmentation for the analysis of array-based DNA copy number data. *Biostatistics* 5 (4), 557–572.
- Picard, F., Robin, S., Lavielle, M., Vaisse, C., Daudin, J., 2005. A statistical approach for array CGH data analysis. *BMC Bioinformatics* 6 (1), 27.
- Pinkel, D., Segraves, R., Sudar, D., Clark, S., Poole, I., Kowbel, D., Collins, C., Kuo, W., Chen, C., Zhai, Y., et al., 1998. High resolution analysis of DNA copy number variation using comparative genomic hybridization to microarrays. *Nature Genetics* 20, 207–211.
- Rabiner, L., 1989. A tutorial on hidden Markov models and selected applications in speech recognition. In: *Proceedings of the IEEE*. Vol. 77. IEEE, pp. 257–286.
- Redon, R., Ishikawa, S., Fitch, K., Feuk, L., Perry, G., Andrews, T., Fiegler, H., Shapero, M., Carson, A., Chen, W., et al., 2006. Global variation in copy number in the human genome. *Nature* 444 (7118), 444–454.

- Rigaill, G., Lebarbier, E., Robin, S., 2011. Exact posterior distributions and model selection criteria for multiple change-point detection problems. *Statistics and Computing*, 1–13.
- Schwarz, G., 1978. Estimating the dimension of a model. *The Annals of Statistics* 6 (2), 461–464.
- Shah, S., Cheung, K., Johnson, N., Alain, G., Gascoyne, R., Horsman, D., Ng, R., Murphy, K., et al., 2009. Model-based clustering of array CGH data. *Bioinformatics* 25 (12), i30.
- Shen, Y., Gu, Y., Pe'er, I., 2011. A Hidden Markov Model for Copy Number Variant prediction from whole genome resequencing data. *BMC Bioinformatics* 12 (Suppl 6), S4.
- Snijders, A., Nowak, N., Segraves, R., Blackwood, S., Brown, N., Conroy, J., Hamilton, G., Hindle, A., Huey, B., Kimura, K., et al., 2001. Assembly of microarrays for genome-wide measurement of DNA copy number by CGH. *Nature Genetics* 29, 263–264.
- StAAF, J., Lindgren, D., Vallon-Christersson, J., Isaksson, A., Goransson, H., Juliusson, G., Rosenquist, R., Hoglund, M., Borg, A., Ringnér, M., 2008. Segmentation-based detection of allelic imbalance and loss-of-heterozygosity in cancer cells using whole genome SNP arrays. *Genome Biol* 9 (9), R136.
- Venkatraman, E., Olshen, A., 2007. A faster circular binary segmentation algorithm for the analysis of array CGH data. *Bioinformatics* 23 (6), 657–663.
- Viterbi, A., 1967. Error bounds for convolutional codes and an asymptotically optimum decoding algorithm. *Information Theory, IEEE Transactions on* 13 (2), 260–269.
- Wang, K., Li, M., Hadley, D., Liu, R., Glessner, J., Grant, S., Hakonarson, H., Bucan, M., 2007. PennCNV: an integrated hidden Markov model designed for high-resolution copy number variation detection in whole-genome SNP genotyping data. *Genome Research* 17 (11), 1665–1674.
- Willenbrock, H., Fridlyand, J., 2005. A comparison study: applying segmentation to array CGH data for downstream analyses. *Bioinformatics* 21 (22), 4084–4091.

Zhang, N., Siegmund, D., 2007. A modified Bayes information criterion with applications to the analysis of comparative genomic hybridization data. *Biometrics* 63 (1), 22–32.